Alumina thin films prepared by direct liquid injection chemical vapor deposition of dimethylaluminum isopropoxide: a process-structure investigation

Loïc Baggetto[*,1], **Jérôme Esvan**[1], **Cédric Charvillat**[1], **Diane Samélor**[1], **Hugues Vergnes**[2], **Brigitte Caussat**[2], **Alain Gleizes**[1], **and Constantin Vahlas**[*,1]

[1] Centre Interuniversitaire de Recherche et d'Ingéniérie des Matériaux (CIRIMAT), Université de Toulouse, 4 allée Emile Monso, BP-44362, 31030 Toulouse Cedex 4, France
[2] Laboratoire de Génie Chimique (LGC), Université de Toulouse, 4 allée Emile Monso, CS-84234, 31432 Toulouse Cedex 4, France

The development of a new process to obtain amorphous alumina thin films is presented. We show for the first time the direct liquid injection chemical vapor deposition (DLI CVD) of alumina thin films using dimethylaluminum isopropoxide (DMAI) precursor in two oxidizing atmospheres. At high process temperature (500-700 °C), the film growth takes place in the presence of O_2 whereas at low temperature (150-300 °C) H_2O vapor is used. The materials characteristics, such as the surface morphology and roughness (SEM and AFM), crystal structure (XRD), composition (EPMA) and chemistry (XPS) are discussed in detail. Very smooth films, with typical roughness values lower than 2.0 nm are obtained. The thin films are all composed of an amorphous material with varying composition. Supported by both EPMA and XPS results, film composition evolves from a partial oxyhydroxide to a stoichiometric oxide at low deposition temperature (150-300 °C) in the presence of H_2O. At higher growth temperature (500-700 °C) in the presence of O_2, the composition changes from that of a stoichiometric oxide to a mixture of an oxide with aluminum carbide.
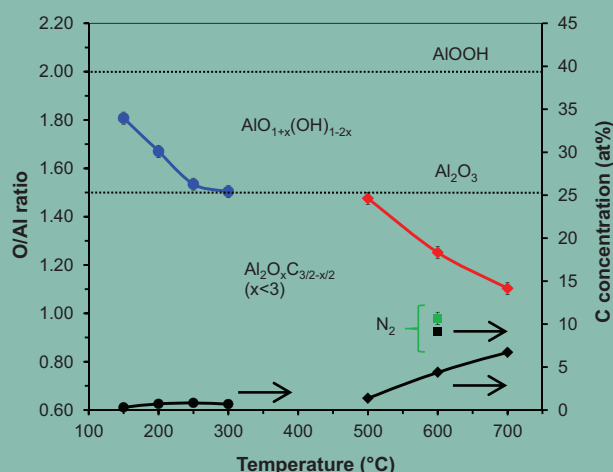
Elemental composition of the alumina films deposited in the presence of H_2O from 150 to 300 °C (circles), in the presence of O_2 from 500 to 700 °C (diamonds) or in the presence of N_2 only at 600 °C (squares). O/Al ratios and C concentrations are shown.

1 Introduction Alumina in the form of powders or coatings is a material of major technological interest for a wide range of applications in optical and microelectronic components, as well as a wear resistance agent and catalyst support, or for the protection against corrosion and high temperature oxidation [1-3]. The protection from corrosion and thermal oxidation of stainless steels, light alloys (Ti- and Mg-based) and composite polymer materials for aero-nautic or automotive applications calls for the development of alumina thin films with superior performances to act as an oxidation barrier for moderate temperature applications (200-600 °C) [4, 5].

Overall, the number of reports on the processing of alumina films is significant. A practical way to produce amorphous alumina thin films is the MOCVD technique [4-9], in which a controlled amount of precursor carried

over a surface decomposes and reacts to form a condensate thin layer. Aluminum tri-isopropoxide (ATI) is a precursor with significant advantages since it is cheap, stable in air and only slowly reactive with water. However, the shelf-life, polymerization and condensation properties of its tetramer pose problems [10] and can lead to tedious reactor maintenance due to line and injector blockage. Furthermore, the applicable range of temperature for ATI is not only limited by the stability window of the substrate but is also constrained by the nature and the elemental composition of the film. Amorphous alumina films grown from ATI are generally hydroxylated for temperatures below 420 °C and have optimal mechanical, corrosion and oxidation protection properties around 520 °C [11, 12]. Trimethyl aluminum (TMA) was also evaluated as a CVD precursor to form alumina films. However, in addition of an oxidizing agent, the process requires the use of a catalytic support or a plasma, and employs deposition temperatures as high if not higher than those employed with ATI [13]. These relatively high temperatures may limit the use of TMA- and ATI-processed alumina films for the protection of materials for which the properties, e.g. mechanical, change importantly above 200 °C. This is the case of Mg alloys and polymer composites.

A few groups proposed the use of dimethylaluminum isopropoxide (DMAI) as an alternative CVD precursor using vaporization in bubbler systems [7, 8, 14-19]. DMAI, which consists of an Al atom linked to 2 methyl and one isopropyl groups, has an intermediate structure between ATI and TMA. Unlike TMA, it is non pyrophoric, and although it is currently more expensive than ATI and is very reactive with water, it presents a significantly higher vapor pressure, it is liquid at room temperature, has a longer shelf-life and is not prone to polymerization. Amorphous alumina films can be deposited from DMAI in the presence of water vapor between 180 and 270 °C, this temperature range being significantly lower than that of ATI processes [8]. Such low deposition temperature paves the way for the protection of light alloys or polymer composite materials. These advantages, combined with the use of a direct liquid injection (DLI) system instead of a bubbler technology for the transport of the precursor in the deposition area make DLI of DMAI an a priori interesting alternative to vaporize ATI in CVD processes. DMAI was also tested for atomic layer deposition (ALD) of alumina [20-24].

In the present work, we discuss for the first time the development of such CVD processes involving DLI of DMAI. The injection system offers several advantages over classical sublimation or evaporation systems since it provides constant precursor vapor flow and leads to a more stable, robust and reproducible process [25-27]. Two oxidizing atmospheres were employed, as selected from former works using evaporation systems [7, 8, 14-19]. Battiston et al. claimed the fabrication of stoichiometric and carbon-free alumina films using O_2 and H_2O oxidizing atmospheres [7, 8] whereas other authors consistently meas-

ured carbon leftovers in their films when using pure N_2 [16-18]. Here, at high deposition temperatures, oxygen has been used to compensate for the lower than 1.5 O/Al ratio in DMAI and to possibly prevent the incorporation of carbon in the films. At lower deposition temperatures, water vapor has been used to compensate for the lack of oxygen in DMAI while promoting the reaction kinetics. The physico-chemical properties of the thin films were characterized using a wide set of techniques. Surface morphology and roughness were measured using scanning electron microscopy (SEM) and atomic force microscopy (AFM). The amorphous state of the films was ascertained by X-ray diffraction (XRD). Elemental compositions as well as the chemical environments of the bulk of the film, with emphasis on the formation of partial hydroxyls or carbides, were determined through X-ray photoelectron spectroscopy (XPS) and electron probe microanalysis (EPMA). EPMA is a powerful probe as it is significantly more precise and accurate than XPS and energy dispersive X-ray spectroscopy (EDS) to determine compositions.

2 Experimental

2.1 Thin film preparation Thin films were prepared using a homemade horizontal hot-wall CVD reactor equipped with three gas lines and mass flow controllers (MFC), a large evaporation stainless steel chamber and a quartz tube (25 mm diameter, 300 mm length) heated by a resistive furnace. A dry pump and pressure gauges connected to the output of the quartz tube were used to control the reaction pressure to 5 Torr. Gas lines and the evaporation steel chamber were heated to *ca.* 80 °C to prevent precursor condensation. One gas line was connected to the injection system consisting of a N_2-pressurized Schlenk flask filled with the precursor solution and connected to a DLI equipment set of two injectors (Kemstream), one for liquid injection and one for gas mixing. The precursor solution was prepared in a Schlenk flask inside a glovebox circulated with purified Ar (99.9997%, Air Products) by adding a known amount of DMAI solution (>99%, Air Liquide) into the flask. The sealed flask was taken out of the glovebox and completed with the appropriate quantity of anhydrous cyclohexane (99.5%, H_2O<10 ppm, Sigma-Aldrich) using an air-tight, Ar-purged, glass syringe to prepare a solution of 0.2 M DMAI. Then, the Schlenk flask was connected to the injection system and purged several times with pressurized N_2 (99.9999%, Praxair). The frequency and opening times of the injection system were controlled to feed the evaporation chamber with small precursor solution droplets mixed with N_2 gas with a flow set from 300 to 450 sccm. For the low temperature process, 120 sccm of N_2 was bubbled through deionized H_2O (> 20 MΩ.cm) kept at room temperature. For the high temperature process, 50 sccm of O_2 (99.9995%, Air Products) was added to the dilution gas (300-400 sccm) installed on the third gas line. In both cases, the oxidants were in large excess compared

to DMAI. Silicon samples (10x10 mm) cut from 4" Si (001) wafers (Sil'tronix) were placed on a stainless steel holder in the center of the quartz tube where the temperature was uniform. Growth conditions for both the low and high temperature processes are listed in Table 1.

2.2 Materials characterization The film thickness was measured using optical reflectivity (Mikropack, Nanocalc 2000). Thickness was confirmed by measuring the film thickness in SEM cross-sections. Samples surface morphology and roughness were measured using SEM and AFM. SEM micrographs were taken in backscattered mode on a JEOL JSM-7800F field emission scanning electron microscope operated at 10 kV. Samples measured with SEM were fractured then covered by a thin layer of sputtered platinum to prevent charging effects. AFM was used in ambient conditions on an Agilent Technologies 5500. Scanning was performed in contact mode with tips of spring constant of about 0.292 N m^{-1} (AppNano). Scanning rate was set to 2 μm s^{-1}. Images were processed with the software Pico Image (Agilent Technologies). The film crystalline structure was measured by XRD on a Bruker D8 Advance using a Cu K$_\alpha$ (1.5418 Å) X-ray tube operated at 40 kV and 40 mA, a Ni filter and solid-state Lynxeye detector in θ+3°/θ-3° configuration. Samples were measured on a zero background holder and a θ offset of 3° was applied between the X-ray source and detector arms to suppress the strong (004) diffraction of the samples Si substrates normally measured around 69° (Fig. S1, see Supporting Information, online at: www.pss-c.com). EPMA was used to accurately determine the O/Al ratios in the films. Characterization was conducted with a Cameca SXFive apparatus operated at 10 and 15 keV and calibrated using a high purity alumina standard. Samples were covered by a thin layer of carbon inside an evaporation chamber (Leica) to prevent charging effects. Each sample was measured 4 to 6 times in different locations to determine the spatial homogeneity of the sample composition.

Table 1 Typical DLI MOCVD process parameters used during the preparation of alumina thin films. DMAI precursor, cyclohexane solvent and a total pressure of 5 Torr were used in all cases.

Temperature (°C)	Reactive gas	Injection mixing flow (sccm)	Dilution flow (sccm)	Growth rate (μm/h)
150	H_2O	300	300	0.4
200	H_2O	300	300	0.6
250	H_2O	300	300	1.1
300	H_2O	300	300	1.8
500	O_2	400	400	0.3
600	O_2	400	400	1.2
600	N_2	450	400	0.9
700	O_2	400	400	2.5

XPS measurements were performed on a Thermo Scientific K-Alpha instrument using monochromatic Al K$_\alpha$ (1486.6 eV) capable of a base pressure of 10^{-9} Torr or less, and equipped with a detector positioned at 90° with respect to the sample surface. The spectrometer energy calibration was performed using the Au4f7/2 (83.9 ± 0.1 eV) and Cu2p3/2 (932.7 ± 0.1 eV) photoelectron lines. Charging compensation and neutralization were applied by using a dual beam flood gun. The probed areas were about 400 μm diameter. A survey scan was collected before and after surface erosion to measure the composition and check for possible contaminants. Surface erosion was employed using Ar ions accelerated at 2 kV, resulting in an erosion rate of about 0.08 nm s^{-1}. Constant pass energy of 30 eV and energy steps of 0.1 eV were used for high resolution scans. The energy scale was fixed by setting the adventitious carbon C1s energy to 284.4 eV. The photoelectron peaks were analyzed by Gaussian/Lorentzian (G/L = 70/30) peak fitting and using a Shirley background. The atomic concentrations were determined from photoelectron peak areas using the atomic sensitivity factors reported by Scofield, taking into account the transmission function of the analyzer. This function was calculated at different pass energies from Ag3d and AgMNN peaks collected for a silver reference sample. C concentrations, reported from these quantifications, are estimated to be exact within ± 20%.

3 Results and discussion AFM derived surface morphology and roughness of two films grown at 200 °C and 600 °C are presented in Fig. 1, and the corresponding roughness parameters are listed in Table 2. It is clear from the AFM data that the two films are extremely smooth, with typical roughness values of about 1.0 nm for the film grown at 200 °C with H_2O, and around 1.5 nm for the film grown at 600 °C with O_2. The film grown at the higher temperature shows somewhat smaller domains and a slightly higher surface roughness. In both cases, the low roughness and absence of nodules support the absence of homogeneous gas phase reactions. Moreover, the low roughness values suggest the formation of a high density of nucleation centers during the film growth, as was proposed to explain the smoothness of alumina films prepared at low temperatures by evaporation of DMAI [8].

Table 2 AFM-derived roughness parameters (nm) of alumina films prepared at 200 °C in the presence of H_2O and at 600 °C in the presence of O_2 (Fig. 1). R_a and R_q stand for the arithmetic and root mean squared roughness of a line profile, respectively. S_a and S_q stand for the areal arithmetic and root mean squared roughness of an entire area scan, respectively. Values are in nm.

| Temperature (°C)	Reactive gas	R_a	R_q	S_a	S_q
200	H_2O	0.93	1.13	0.94	1.23
600	O_2	1.57	1.95	1.35	1.71

The results obtained at high temperatures contrast with those reported for alumina films prepared at high temperatures by evaporation of DMAI [7], where significantly rougher films were obtained. This difference might result from the lower growth rate used in our work, which gives surface diffusion and atomic rearrangement more time to take place.
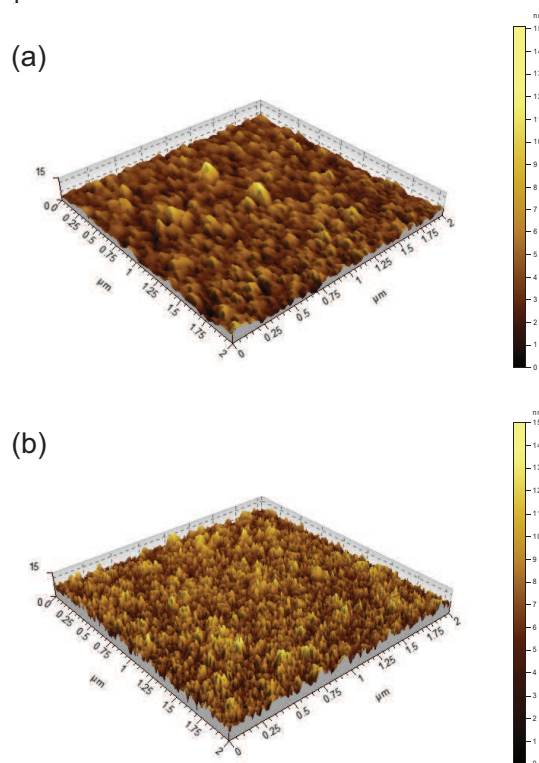

Figure 1 3D topography images of the surfaces measured by contact AFM for alumina films deposited onto Si substrates at (a) 200 °C in the presence of H_2O and at (b) 600 °C in the presence of O_2. Film thicknesses are 440 and 720 nm, respectively. The roughness parameters derived from the measurements are listed in Table 2.

The samples surfaces imaged by SEM are shown in Fig. 2. As observed with AFM, the films are extremely smooth, without any pinholes and look dense. The measurement of the film thickness in the cross-section views was found to be in very good agreement with the optical reflectivity measurements, with deviations of about 5%.

The amorphous structure of the thin film materials was ascertained by XRD for all deposition temperatures in both oxidizing atmospheres. The diffraction patterns (Fig. 3) do not show any peaks associated with the formation of a crystalline structure. The absence of significant broad humps, except that of the Si substrate near 69° (cf. Fig. S1 of the Supporting Information) suggests the formation of amorphous thin film materials, similar to the results of former works concerning the deposition of alumina films from DMAI [7, 8, 14-19] or ATI [4-10, 12] precursors for temperatures up to 700 °C.
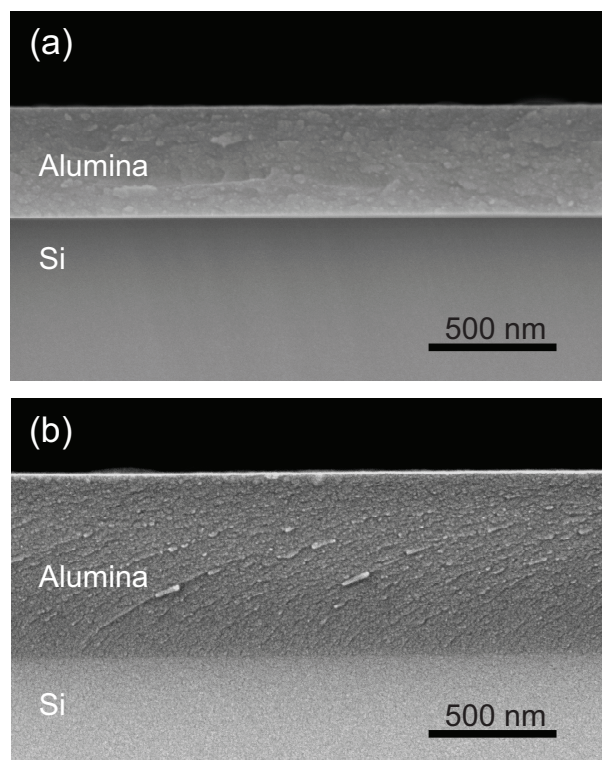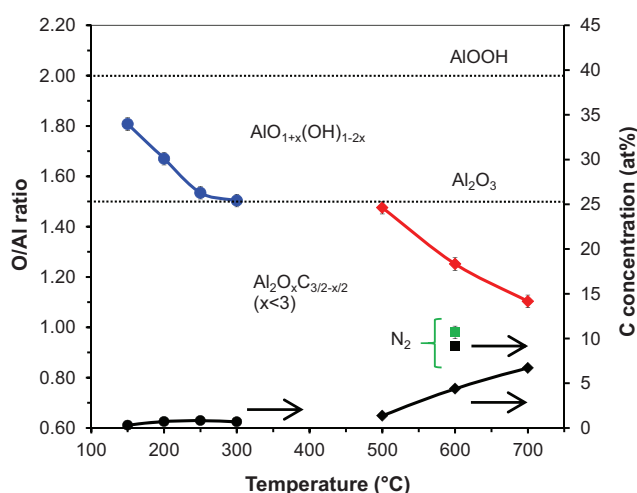

Figure 2 SEM cross-sections of the alumina films deposited onto Si substrates at (a) 200 °C in the presence of H_2O and at (b) 600 °C in the presence of O_2. Film thicknesses are *ca.* 440 and 720 nm, respectively.
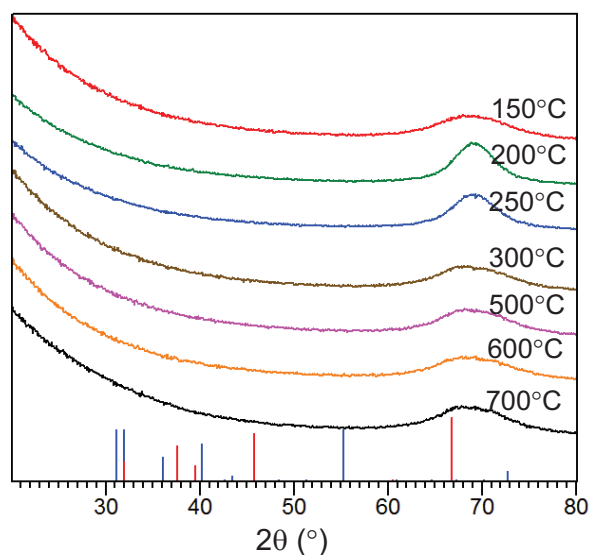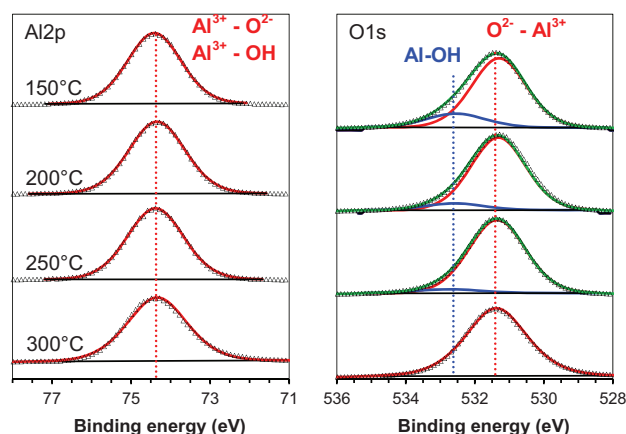

Figure 3 XRD patterns for alumina thin films deposited in the presence of H_2O for substrate temperatures from 150 to 300 °C and in the presence of O_2 for substrate temperatures from 500 to 700 °C. The broad humps around 69° result from the Si substrate in the 3° θ offset configuration (see Experimental section and Fig. S1). Red and blue vertical bars represent the reference patterns of γ-Al_2O_3 and Al_4C_3.

In the absence of XRD phase identification, we investigated the composition of the films using XPS (after systematic erosion of a *ca.* 100 nm surface layer) and EPMA. EPMA is a powerful probe to measure the O/Al with exactness and precision using internal standards. The O/Al ratios obtained from EPMA measurements are compared to the ratios expected for AlOOH and Al_2O_3 references. The films prepared at 150 and 200 °C in the presence of H_2O vapor show O/Al atomic ratios of 1.81 and 1.67, respectively (Fig. 4). These values are comprised between those of AlOOH (2.0) and Al_2O_3 (1.5), thus revealing partially hydroxylated alumina $AlO_{1+x}(OH)_{1-2x}$. The films prepared at 250 and 300 °C show O/Al ratios of 1.54 and 1.50, respectively, in good agreement with the formula Al_2O_3. The C content measured by XPS (Fig. S2, Supporting Information) is below 1 at%. The film prepared at 500 °C in the presence of O_2 has an O/Al ratio of 1.48, which may be ascribed to the formula Al_2O_3. The films prepared at 600 and 700 °C have O/Al ratios of 1.25 and 1.10, well below 1.50. The decrease in O/Al ratio is clearly related to an increase in the C concentration, up to about 6.5 at% in the film prepared at 700 °C, as has been also evidenced by Schmidt et al. during the preparation of alumina films from sublimed DMAI in this temperature range [17, 18]. This suggests the formation of the aluminum carbide Al_4C_3 and/or of aluminum oxycarbides, e.g. Al_4O_4C or Al_2OC [28-31], along with Al_2O_3, to lead to the generic composition of $Al_2O_xC_{3/2-x/2}$. The formation of oxycarbides can be thought to result from the partial substitution of one C^{4-} anion for two O^{2-} anions, leading to the formulas Al_4O_4C, Al_2OC, and ultimately Al_4C_3.

The XPS results for the samples prepared at low temperature using H_2O vapor are presented in Fig. 5. For all samples, the absence of reduced species such as Al_2O_{3-x} or metallic Al signal expected around 73.5 and 72.5 eV in Al2p, respectively, suggests that ion sputtering erosion did not significantly alter the bulk structure of the alumina material. The amount of aliphatic carbon (C-C and C-H bonds, Fig. S2, Supporting Information) is less than 1 at% for all samples. The carbon species likely result from partial decomposition of the precursor or from solvent residues incorporated in the film during growth. The Al2p signal around 74.4 eV apparently shows a single symmetric peak. Its main contribution is from Al^{3+} in an O^{2-} framework. A small proportion overlapping with the main peak (not shown) is thought to result from Al oxyhydroxides, for which the response is expected to be very similar to that of the oxide. Indeed, the signals for Al2p in Al_2O_3, AlOOH and $Al(OH)_3$ are very close in binding energy and hard to separate [32-34]. The O1s signal is a much better discriminant for the presence of hydroxyl groups, which have a peak expected at about 1.3 eV offset from the main O^{2-} peak of Al_2O_3 [33, 34]. The measured O1s signals clearly show a main peak around 531.4 eV at the location expected for O^{2-} in the Al_2O_3 framework [32, 33, 35, 36] accompanied with a shoulder of increasing intensity with decreasing temperature around 532.7 eV attributable to hydroxyl groups. The relative amount of hydroxyl groups increases as the temperature decreases, in excellent agreement with the increasing O/Al ratio measured with EPMA (Fig. 4). In a nutshell, XPS results for films processed at low temperature in the presence of H_2O show the quasi-absence of C and the presence of hydroxyl groups for the lowest deposition temperatures whereas no hydroxyls are detected at 300 °C, in good agreement with the EPMA results.


Figure 4 Elemental composition of the alumina films, using EPMA (O/Al atomic ratios; blue for H_2O, red for O_2, and green for N_2) and XPS (C atomic concentration; black). Films were deposited in the presence of H_2O from 150 to 300 °C (circles), in the presence of O_2 from 500 to 700 °C (diamonds) or in the presence of N_2 only at 600 °C (squares). Each sample was measured with EPMA 4 to 6 times in different locations to check the homogeneity of the composition.

Figure 5 High resolution X-ray photoelectron spectra (Al2p and O1s) of alumina films deposited from 150 to 300 °C in the presence of H_2O. The decomposition of the spectra into the assigned chemical species is shown for each core level.

The XPS results for samples prepared at high temperature in the presence of O_2 are presented in Fig. 6. The Al2p and O1s signals clearly show the presence of intensity at the locations expected for Al_2O_3 with Al2p binding energy of about 74.4 eV and O1s binding energy near 531.5 eV, as discussed above. Moreover, the signals observed at about 73.2 eV in Al2p and near 282.0 eV in C1s are normally attributed to aluminum carbide Al_4C_3 [37, 38]. The Al2p binding energy of aluminum carbide is lower than that measured for Al_2O_3 since C is less electronegative (more electropositive) than O, hence Al in aluminum carbide is more effectively reduced and measured at a lower binding energy. Similarly, the C1s binding energy of the carbide is significantly more negative than that of adventitious C-C bonds as Al is more electropositive than C.
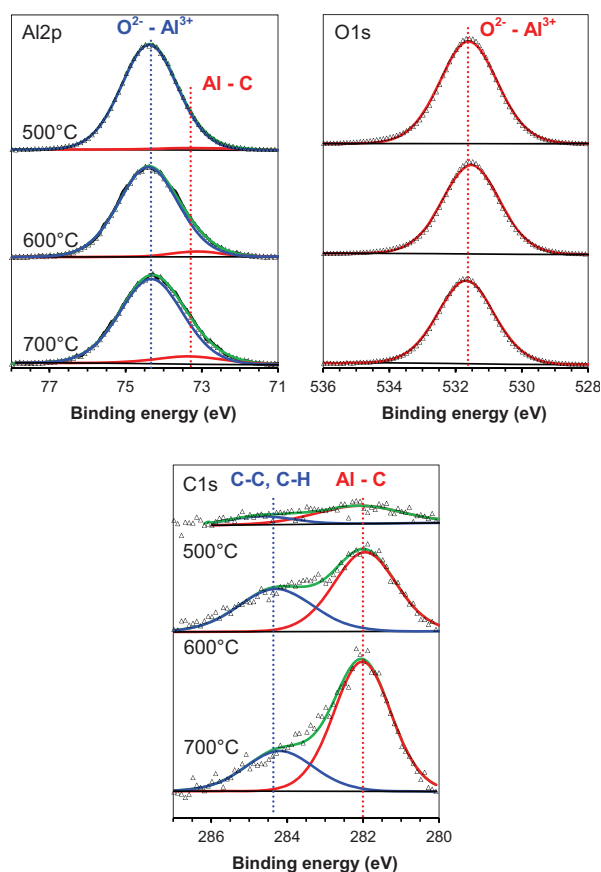
Figure 6 High resolution X-ray photoelectron spectra (Al2p, C1s and O1s) of alumina thin films deposited from 500 to 700 °C in the presence of O_2. The decomposition of the spectra into the assigned chemical species is shown for each core level.

The relative atomic contribution of carbon in aluminum carbide over aliphatic carbon is 75% at 500 °C, 60% at 600 °C and 73% at 700 °C, and the absolute amount of carbon related to the carbides clearly increases with increasing deposition temperature from about 1 at% at 500 °C to about 5 at% at 700 °C. This result is in line with a former report, showing that the CVD from trimethylalu-

minum and methane leads to pure Al_4C_3 films only at temperatures as high as 1150 °C [30]. Here, the presence of aluminum carbides can be the result of the reaction of cyclohexane with the growing alumina film. This is suggested by earlier results that showed the absence of C in films grown at 560 °C during the MOCVD of O_2 and DMAI transported by evaporation [7]. However, other reports showed that C was incorporated in alumina films when using DMAI precursor in N_2 atmosphere [17, 18]. DMAI is composed of 2 C atoms linked to Al, and can by itself be expected to partly contribute to the formation of carbides. It is interesting to note that a sample deposited at 600 °C in pure N_2 (no O_2 added) had a significantly higher C concentration (9.2 at%) with about 75% in the form of aluminum carbides, concomitant with a much lower O/Al ratio (0.98) than for samples deposited in O_2 atmosphere (Fig. 4). This result further strengthens the need to use an oxygen source when employing DMAI precursor in a DLI system to limit the amount of formed aluminum carbides that originate either from the precursor molecule or from the used solvent.

4 Conclusions Direct liquid injection chemical vapor deposition of alumina thin films from DMAI precursor has been investigated for the first time. O_2 as well as H_2O oxidizing environments have been used to assist the formation of Al_2O_3. The produced films are extremely smooth (R_a in the range of 1-2 nm) and have an amorphous structure. The composition of the films evolves from a partial oxyhydroxide $AlO_{1+x}(OH)_{1-2x}$ to Al_2O_3 for films processed at low temperatures (150-300 °C) in the presence of H_2O. The films prepared at higher temperatures (500-700 °C) in the presence of O_2, consist of the oxide Al_2O_3, either pure (500 °C) or mixed with aluminum carbide (600 and 700 °C) in amounts increasing with the temperature.

References

[1] S. Blittersdorf, N. Bahlawane, K. Kohse-Höinghaus, B. Atakan, and J. Müller, Chem. Vap. Depos. **9**, 194 (2003).
[2] V.A.C. Haanappel, H.D. van Corbach, R. Hofman, R.W.J. Morssinkhof, T. Fransen, and P.J. Gellings, High Temp. Mater. Processes **15**, 245 (1996).
[3] S.S. Yom, W.N. Kang, Y.S. Yoon, J.I. Lee, D.J. Choi, T.W. Kim, K.Y. Seo, P.H. Hur, and C.Y. Kim, Thin Solid Films **213**, 72 (1992).

[4] A.-M. Lazar, W. P. Yespica, S. Marcelin, N. Pébère, D. Samélor, C. Tendero, and C. Vahlas, Corros. Sci. **81**, 125 (2014).

[5] S. Krumdieck, S. Davies, C. M. Bishop, T. Kemmitt, and J. V. Kennedy, Surf. Coat. Technol. **230**, 208 (2013).

[6] F. Wiest, V. Capodieci, O. Blank, M. Gutsche, J. Schulze, I. Eisele, J. Matusche, and U. I. Schmidt, Thin Solid Films **496**, 240 (2006).

[7] D. Barecca, G. A. Battiston, R. Gerbasi, and E. Tondello, J. Mater. Chem. **10**, 2127 (2000).

[8] G. A. Battiston and R. Gerbasi, Chem. Vap. Depos. **8**, 193 (2002).

[9] Y. Balcaen, N. Radutoiu, J. Alexis, J.-D. Beguin, L. Lacroix, D. Samélor, and C. Vahlas, Surf. Coat. Technol. **206**, 1684 (2011).

[10] M.-M. Sovar, D. Samélor, A. N. Gleizes, and C. Vahlas, Surf. Coat. Technol. **201**, 9159 (2007).

[11] A. N. Gleizes, C. Vahlas, M.-M. Sovar, D. Samélor, and M.-C. Lafont, Chem. Vap. Depos. **13**, 23 (2007).

[12] V. Sarou-Kanian, A. N. Gleizes, P. Florian, D. Samélor, D. Massiot, and C. Vahlas, J. Phys. Chem. C **117**, 21965 (2013).

[13] Y.-I. Ogita and N. Saito, Thin Solid Films, **575**, 47 (2015).

[14] W. Koh, S.-J. Ku, and Y. Kim, Thin Solid Films **304**, 222 (1997).

[15] S. Y. Lee, B. Luo, Y. Sun, and J. M. White, Y. Kim, Appl. Surf. Sci. **222**, 234 (2004).

[16] G. Carta, M. Casarin, N. El Habra, M. Natali, G. Rossetto, C. Sada, E. Tondello, and P. Zanella, Electrochim. Acta **50**, 4592 (2005).

[17] B. W. Schmidt, B. R. Rogers, W. J. Sweet III, C. K. Gren, and T. P. Hanusa, J. Eur. Ceram. Soc. **30**, 2301 (2010).

[18] B. W. Schmidt, B. R. Rogers, C. K. Gren, and T. P. Hanusa, Thin Solid Films **518**, 3658, (2010).

[19] S. S. Lee, E.-S. Lee, S. H. Kim, B. K. Lee, S. J. Jeong, J. H. Hwang, C. G. Kim, T.-M. Chung, and K.-S. An, Bull. Korean Chem. Soc. **33**, 2207 (2012).

[20] K.-S. An, W. Cho, K. Sung, S. S. Lee, and Y. Kim, Bull. Korean Chem. Soc. **24**, 1659 (2003).

[21] W. Cho, K. Sung, K.-S. An, S. S. Lee, T.-M. Chung, and Y. Kim, J. Vac. Sci. Technol. A **21**, 1366, (2003).

[22] S. E. Potts, G. Dingemans, C. Lachaud, and W. M. M. Kessels, J. Vac. Sci. Technol. A **30**, 021505 (2012).

[23] Y. Wu, S. E. Potts, P. M. Hermkens, H. C. M. Knoops, F. Roozeboom, and W. M. M. Kessels, Chem. Mater. **25**, 4619 (2013).

[24] J. Yang, B. S. Eller, M. Kaur, and R. J. Nemanich, J. Vac. Sci. Technol. A **32**, 021514 (2014).

[25] M. Manin, S. Thollon, F. Emieux, G. Berthome, M. Pons, and H. Guillon, Surf. Coat. Technol. **200**, 1424 (2005).

[26] J. Mungkalasiri, L. Bedel, F. Emieux, J. Doré, F. N. R. Renaud, and F. Maury, Surf. Coat. Technol. **204**, 887 (2009).

[27] P. L. Etchepare, H. Vergnes, D. Samélor, D. Sadowski, C. Brasme, B. Caussat, and C. Vahlas, Adv. Sci. Technol. **91**, 117 (2014).

[28] L. M. Foster, G. Long, and M. S. Hunter, J. Am. Ceram. Soc. **39**, 1 (1956).

[29] J. M. Lihrmann, T. Zambetakis, and M. Daire, J. Am. Ceram. Soc. **72**, 1704 (1989).

[30] Y. Ozcatalbas, Compos. Sci. Technol. **63**, 53 (2003).

[31] D. Kima, Y. Onishi, R. Oki, and S. Sakai, Thin Solid Films **557**, 216 (2014).

[32] H. He, K. Alberti, T. L. Barr, and J. Klinowski, J. Phys. Chem. **97**, 13703 (1993).

[33] A. Hess, E. Kemnitz, A. Lippitz, W. E. S. Unger, and D.-H. Menz, J. Catalysis **148**, 270 (1994).

[34] J. T. Kloprogge, L. V. Duong, B. J. Wood, and R. L. Frost, J. Colloid Interf. Sci. **296**, 572 (2006).

[35] S. Verdier, L. El Ouatani, R. Dedryvère, F. Bonhomme, P. Biensan, and D. Gonbeau, J. Electrochem. Soc. **154**, A1088 (2007)

[36] L. Baggetto, N. J. Dudney, and G. M. Veith, Electrochim. Acta **90**, 135 (2013).

[37] R. Hauert, J. Patscheider, M. Tobler, and R. Zehringer, Surf. Sci. **292**, 121 (1993).

[38] B. Maruyama and F. S. Ohuchi, J. Mater. Res. **6**, 1131 (1991).